Project No. 11-2982

A Research Program for Fission Product/Dust Transport in HTGR's

Reactor Concepts

Sudarshan Loyalka
University of Missouri, Columbia

Madeline Feltus, Federal POC
Paul Humrickhouse, Technical POC

NEUP Nuclear Energy University Programs
U.S. Department of Energy

FINAL REPORT-NEUP 2982

A Research Program for Fission Product/Dust Transport in HTGR's

PI: Sudarshan K. Loyalka
Nuclear Science & Engineering Institute,
University of Missouri, Columbia, MO 65211
loyalkas@missouri.edu; 573-882-3568

Associated Faculty (Co-PIs, all at University of Missouri):
J. Brockman, T. K. Ghosh, M. Greenlief
W. H. Miller, J. D. Robertson, R. V. Tompson, D. S. Viswanath,

PhD Students and Post-Doctoral Associates:
L. Carter, M. Reining, JD Seelig, M. Simones, N. White,
J. Jeong, Z. Smith,

Collaborators:
N. S. Jacobson
Glenn Research Center, NASA, Cleveland, Ohio

Duration: September 2011 – September 2015
Submitted February, 2016

Table of Contents

Summary

High and Very High Temperatures Gas Reactors (HTGRs/VHTRs) have five barriers to fission product (FP) release: the TRISO fuel coating, the fuel elements, the core graphite, the primary coolant system, and the reactor building. This project focused on measurements and computations of FP diffusion in graphite, FP adsorption on graphite and FP interactions with dust particles of arbitrary shape.

Diffusion Coefficients of Cs and Iodine in two nuclear graphite were obtained by the release method and use of Inductively Coupled Plasma- Mass Spectroscopy (ICP-MS) and Instrumented Neutron Activation Analysis (INAA). A new mathematical model for fission gas release from nuclear fuel was also developed.

Several techniques were explored to measure adsorption isotherms, notably a Knudsen Effusion Mass Spectrometer (KEMS) and Instrumented Neutron Activation Analysis (INAA). Some of these measurements are still in progress. The results will be reported in a supplemental report later.

Studies of FP interactions with dust and shape factors for both chain like particles and agglomerates over a wide size range were obtained through solutions of the diffusion and transport equations. The Green's Function Method for diffusion and Monte Carlo technique for transport were used, and it was found that the shape factors are sensitive to the particle arrangements, and that diffusion and transport of FPs can be hindered. Several journal articles relating to the above work have been published, and more are in submission and preparation.

NEUP_2982_Final Report (2016)

Project Title: A research program for fission product/dust transport and adsorption/deposition in HTGRs

Technical Work Scope Identification: NGNP-1

Project Scope and Description

The Next Generation Nuclear Plant (NGNP) will be a Nuclear Regulatory Commission (NRC) licensed commercial high temperature gas-cooled reactor (HTGR or VHTR) plant (prismatic or pebble bed) capable of producing electricity and high temperature process heat. The DOE position on the NRC approval for HTGR licensing is described in a recent document, Mechanistic Source Terms White Paper, INL/EXT-10-17997, July 2010, and will follow 10 CFR 52. HTGRs have five barriers to fission product release: the TRISO fuel coating, the fuel elements, the core graphite, the primary coolant system, and the reactor building. Figure 1 (from the aforementioned report) describes paths to the source term for a prismatic HTGR. Similar paths apply to the pebble bed reactors also (with additional dust from pebble abrasion). The radionuclides of main interest are tritium, noble gases, halogens (^{131}I), alkali metals, tellurium group metals, alkaline earth metals, and noble metals.

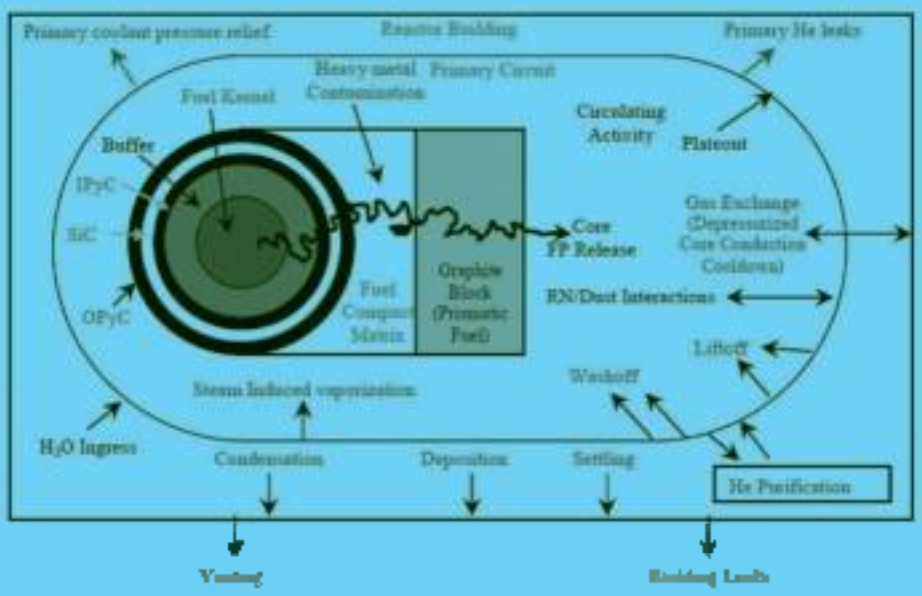

Figure 1. HTGR radionuclide retention system

The computations are to take advantage of the other four retentive barriers for the normal conditions, as well as to address the factors that lead to the releases, and contribute to the source terms during the accident conditions. Table 1 describes some interactions of various fission products (FPs) both

in-core and ex-core. The report emphasizes needs for new data and computations for FP diffusion and adsorption, and interactions with dust. It notes, for example, that,

"The quantities and form of dust in current designs for HTGRs are unknown … Correlations are needed that give the sorptivities of these nuclides as a function of temperature, partial pressure, surface state, and coolant chemistry for normal operating and accident conditions."

Table 1: Interaction of fission products both in-core and ex-core.

Radionuclide Class	Key Nuclide	Form in Fuel	Principal In-Core Behavior	Principal Ex-Core Behavior
Tritium	^{3}H	Gas	Permeates intact SiC; sorbs on core graphite	Permeates through heat exchangers
Noble gases	^{135}Xe	Gas	Retained by PyC/SiC	Removed by helium purification system
Halogens	^{131}I	Gas	Retained by PyC/SiC	Deposits on colder metals
Alkali metals	^{137}Cs	Oxide-element	Retained by SiC; some matrix/graphite retention	Deposits on metals/dust
Tellurium group	^{132}Te	Complex	Retained by PyC/SiC	Deposits on metals/dust
Alkaline earths	^{90}Sr	Oxide-carbide	High matrix/graphite retention	Deposits on metals/dust
Noble metals	^{110m}Ag	Elemental	Permeates intact SiC	Deposits on metals

Our objectives (tasks) in this research are to focus specifically on experiments and computations to identify phenomena of interest and to model FP transport and adsorption, and dust/aerosol facilitated FP transport. Towards these, we have accomplished what is outlined (but not limited to) in this report.

Task 1: Computation & Measurement of Diffusion through Graphite

The objective for Task 1 is to undertake computations and measurements of fission product (FP) diffusion through graphite, which will be normally encountered during the high temperature operational phase of HTGRs/VHTRs.

After several different considerations, and initial explorations, we decided to use the release method to obtain diffusion coefficients of FPs in different graphitic species at characteristic HTGR temperatures.

We note that the release and profile methods that were used previously for measurements of diffusion coefficients of Cs and other FP diffusants in graphite. In these works graphite samples were impregnated with FP material, and then annealed at specified temperatures and for certain time periods to effect FP release. These techniques involved radioanalytical measurements of initial and final FP concentration in the graphite sample (release method), or the concentration profile by sectioning of the sample (profile method). The diffusion coefficients were then extracted from the data by comparison with theoretical results as given by the diffusion equation. Additionally, in one case the release rates of ^{134}Cs from a sphere were measured using gamma spectrometry, and the diffusion coefficient was extracted by comparing this rate to the theoretical expression for the release rate.

We have used inductively coupled plasma-mass spectrometry (ICP-MS) to measure FP release rates from graphite spheres or cylinders infused with Cs, and also calibrated and verified the results against Instrumented Neutron Activation Analysis (INAA) when appropriate. The method is general, and can be applied to measurements of diffusion coefficients of several substances or mixtures of substances as well.

For our purposes here, the diffusion of a species in a sample is generally described by the equations:

$$\frac{\partial C(\mathbf{r},t)}{\partial t} = D\nabla^2 C(\mathbf{r},t)$$
$$C(\mathbf{r},0) = C_0$$
$$C(\mathbf{r}_s,t) = 0$$

Where, $C(\mathbf{r},t)$ is the fission product concentration (g/m^3), D is the diffusion coefficient (m^2/s), r is the radial coordinate (m), $\mathbf{r}$ is the distance vector (m), and t is the time (s). C_0 is the initial uniform concentration (g/m^3), although one can consider spatially dependent cases also. Additionally, we take the ansatz that $C(\mathbf{r},t)$ is finite everywhere. One determines the diffusion coefficient D by comparing some experimental data (usually the fractional release rate, $f(t)$, or the cumulative fractional release $F(t)$) with the corresponding theoretical results. The release rates are defined as:

$$f(t) = \frac{1}{VC_0}\int\left(-D\frac{\partial C(\mathbf{r}_s,t)}{\partial \mathbf{n}}\right)dS$$

And,

$$F(t) = \int_0^t f(t')dt'$$

Where V is the volume of the sample, and $\mathbf{n}$ is a unit normal vector at $\mathbf{r}$, a point on the surface and is directed outwards from the body. Convenient series expansions (for short time frames) for spherical or cylindrical geometries are available in the literature, and can also be constructed as needed for differing initial assumptions.

In one particular set of experiments, we used IG-110 manufactured by Toyo Tanso. IG-110 is produced using an isostatic rubber press process and is semi-isotropic. Spherical samples were milled to a radius of 0.2 cm. The spheres were impregnated with cesium using a modified procedure that was adapted from Hayashi and Fukuda. Ten graphite spheres were loaded into a quartz vial (0.6 cm diameter, 4 cm length) with 600 µg of Cs in the form of $CsNO_3$. The vial was then sealed under a low vacuum (40 mTorr). By heating the sample to 500°C the nitrate salt is principally converted to elemental Cs.

After 1 hour, the temperature was increased to 1100°C and maintained for 99 hours to uniformly distribute the cesium throughout the graphite. The temperature was reduced at a rate of 1°C/min until the oven temperature was 200°C. The spheres were removed from the vial and reduced to a final radius of 0.15 cm using SiC sandpaper. The purpose of reducing the radius from 0.2 cm to 0.15 cm was to remove any Cs which may have condensed onto the spheres during the cooling period in the oven.

The initial mass of Cs in each sphere was measured using instrumental neutron activation analysis (INAA). Comparator standards were prepared from a certified solution of $CsNO_3$ purchased from High Purity standards. A 50 µL aliquot of the standard solution was pipetted onto filter paper placed in a high density polyethylene vial with a volume of 200 µL. The standards were dried and capped with friction fit caps. The graphite spheres and comparator Cs standards were irradiated in the rotary 2 pneumatic tube irradiation position of MURR for 30 seconds in a neutron flux of 5.0×10^{13} n/(cm^{2}s). The 127.5 keV gamma line from the decay of ^{134m}Cs produced by the reaction ^{133}Cs(n,g)^{134m}Cs was measured by counting the sample 2.5 cm from the face of a HPGe detector. The samples were counted until at least 10,000 counts were measured from the 127.5 keV photopeak. The initial mass of Cs in the 10 graphite spheres ranged from 12.2 µg to 16.1 µg.

The release experiment is carried out inside of a SiC tube mounted in a Lindberg tube furnace. A diagram of the experimental apparatus is shown in figure 1.

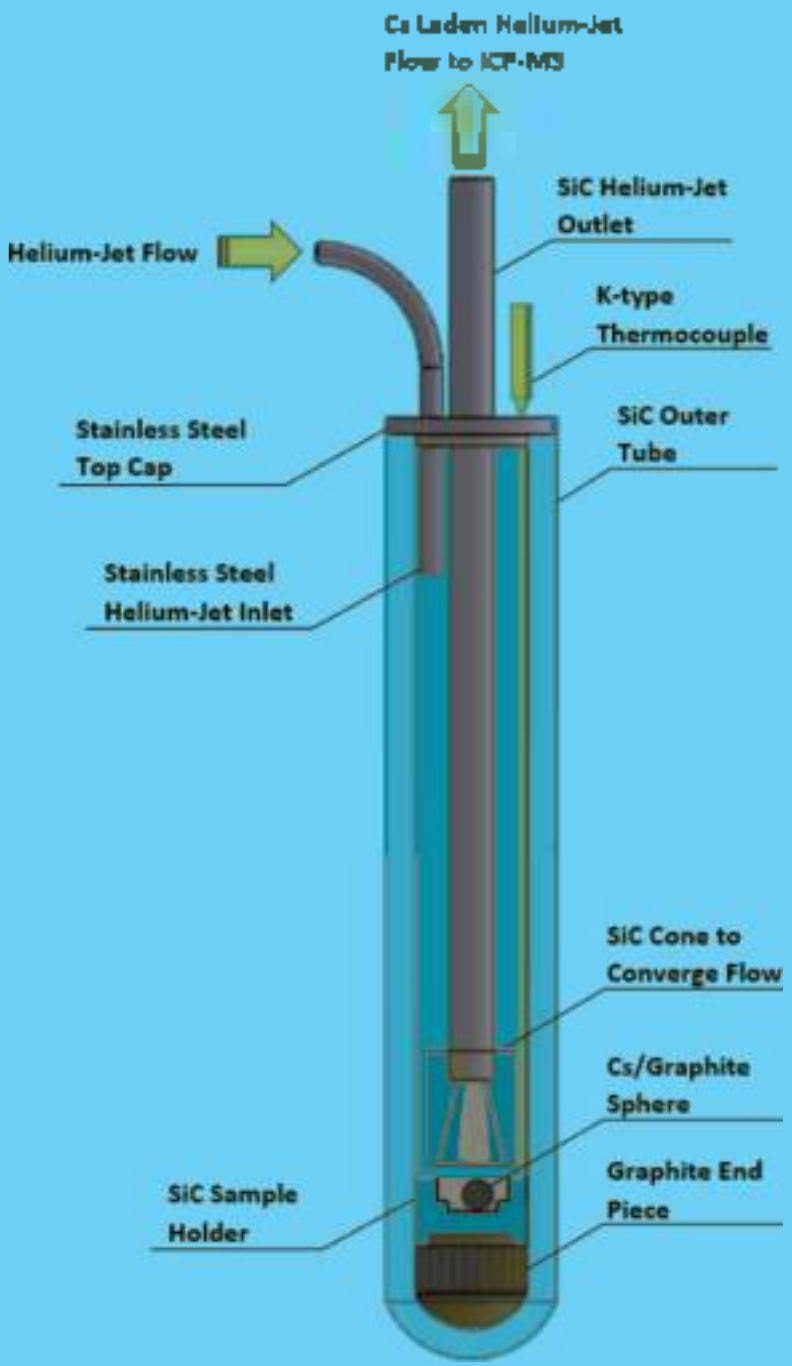

Figure 2. The release experiment takes place inside SiC tube that is closed at one end and mounted vertically in a Lindberg tube furnace. The arrows show the helium jet path.

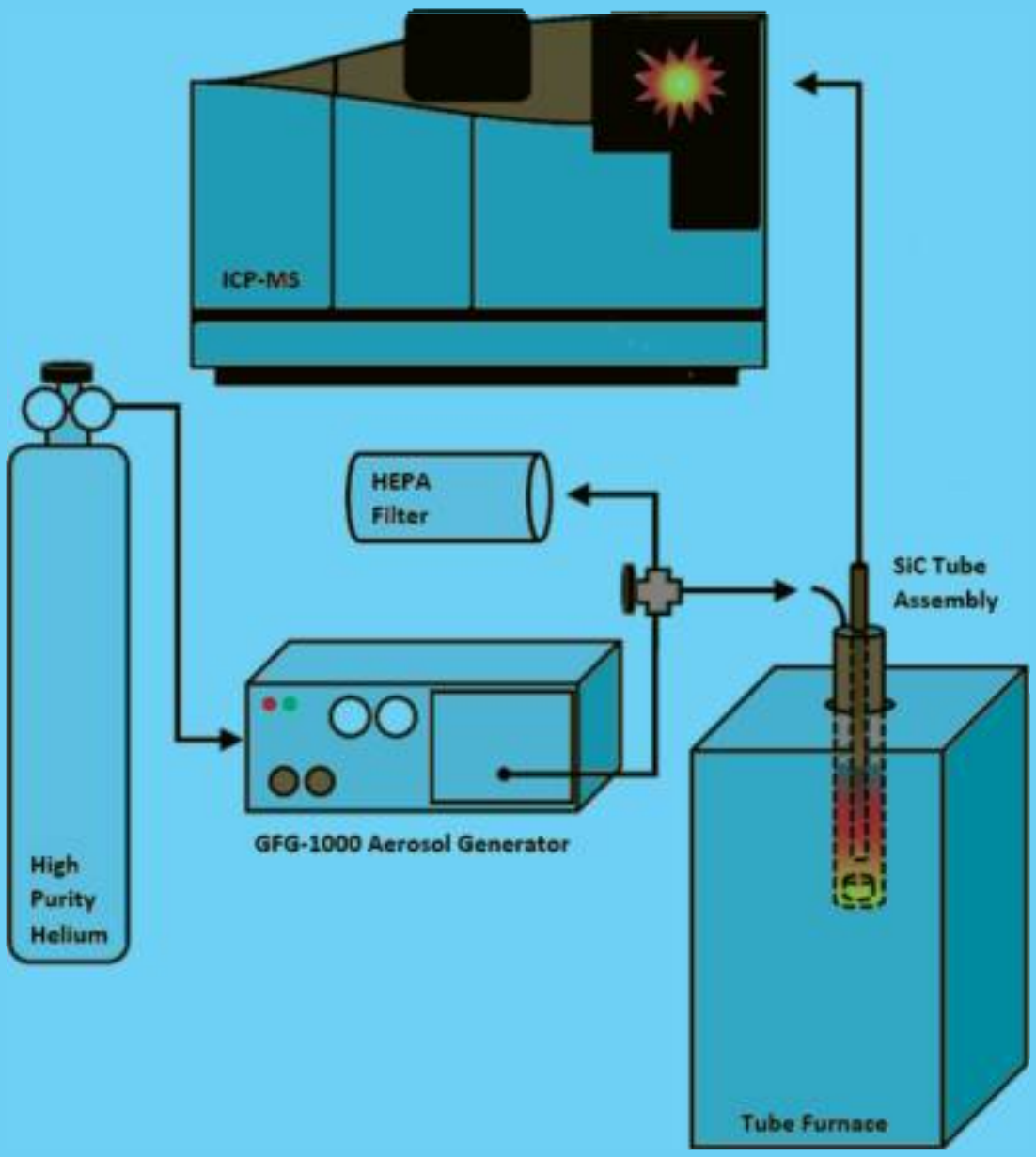

Figure 3. Schematic of the release experiment setup. The graphite sphere is located inside the SiC tube. Cs that is released is transported to the ICP-MS by a He-jet system.

The tube furnace heats the sample region of the SiC tube assembly to the target temperature. The top 10 cm of the SiC tube extends out of the tube furnace and is accessible. The temperature at the SiC holder is monitored using a K-type thermocouple. At the start of an experiment a room temperature graphite sphere containing a known mass of Cs is dropped into the heated sample holder. A sample holder constructed of SiC sits at the bottom of the assembly and holds the graphite sphere. The Cs released from the graphite sphere is transported from the diffusion chamber to an online ICP-MS for real time analysis using a carbon aerosol helium gas jet system.

A gas jet uses particles entrained in flowing gas to transport elements over long distances at room temperature. The helium jet built for this experiment was modeled after the system used at the TRIGA reactor in Mainz, Germany which uses carbon nanocrystals. A modified Palas GFG 1000 carbon aerosol generator was used to produce carbon particles with diameter lognormally distributed around 50 nm. The aerosol generator functions by creating a spark discharge between two graphite electrodes which vaporizes carbon at the electrode surfaces. The vaporized carbon condenses into carbon particles entrained in helium that flows between the graphite electrodes at 4 L/min. The carbon aerosol laden helium is introduced into the SiC tube assembly using the He-jet inlet tube shown in figure 3. The path of the helium jet inside the SiC tube assembly is illustrated in figure 1 by the orange arrows. The helium jet flows around the graphite sphere where released Cs sorbs onto the carbon particles. The Cs laden helium jet exits the SiC tube and travels through a 3 m stainless steel tube that connects to a Perkin Elmer Nexion 300X ICP-MS via a two port quartz spray chamber, shown in figure 4. The other port of the spray chamber contains a liquid nebulizer which continuously introduces a standard solution of 1.00 ng/g indium. The indium is used as an internal standard to monitor and correct for instrument drift over the course of the experiment. The helium jet operates for up to 6 hours during the experiment.

Figure 4: Dual inlet spray chamber. Inlet 1 (left) from He-jet with He flow rate of 1 L/min. Inlet 2 (right) from nebulizer that injects 200 µL/min of 1.00 ng/g In as an internal standard.

At the start of an experiment, the SiC tube assembly is heated to the target temperature. The helium-jet system is turned on and the ICP-MS is started, tuned, and set to collect data for 30-60 minutes prior to introduction of the graphite sphere. Prior to sample introduction residual Cs on the SiC tube assembly surfaces is released and transported by the helium-jet to the ICP-MS detector. This constitutes a detector background of Cs. The background is monitored until it represents less than 1% of the expected Cs count rate. The He-jet outlet tube is disconnected while the SiC tube assembly is at the target temperature and the graphite sphere is dropped inside and, by gravity, descends into the SiC tube sample holder. The sphere is positioned as shown in the cutout section of figure 2.

Diffusion coefficients are computed by measuring cumulative mass release or release rate from the graphite sphere as a function of time using ICP-MS. The value of the diffusion coefficient follows via a regression analysis.

The ICP-MS output is the count rate of Cs and the internal standard indium measured at the detector. It must be calibrated to produce a signal in units of an actual mass transport rate or quantity. The Cs count rate is scaled to the Cs mass transport rate by multiplication with the calibration factor, $F_{\text{calibration}}\,(g/cnts.)$ which is a ratio of the total mass of Cs which has diffused $m_{\text{diffused}}\,(g)$ in an experiment and the total number of detector counts acquired by the ICP-MS $K_{\text{measured}}\,(cnts.)$ in the same time interval:

$$F_{\text{calibration}} = \frac{m_{\text{diffused}}}{K_{\text{measured}}}$$

The m_{diffused} was calculated as the Cs mass difference of the graphite sphere before and after the diffusion experiment measured by INAA. The calibration factor is used to calculate the release rate $Z_R\,(g/s)$, using the detector count rate $k_{\text{measured}}\,(cnts/s)$ the calibration factor $F_{\text{calibration}}\,(g/cnts.)$ The experimental release rate is:

$$Z_R = k_{\text{measured}} F_{\text{calibration}}$$

Integration of the experimental release rate with respect to time yields the Cs mass diffused, and the experimental fractional release $F_{\text{exp}}(t)$ is the ratio of the mass diffused to the mass initially present in the sphere. For a given experiment, a plot of the $F_{\text{exp}}(t)$ vs. t is fitted with theoretical series or the short time expression via a regression analysis to determine the diffusion coefficient.

The Arrhenius equation is used to describe the temperature dependence of the diffusion coefficient in terms of the pre-exponential factor D_0 (m^2/s) and corresponding activation energy E (J/mol). We have obtained D_0 and E in the temperature range of 1100-1300K from an Arrhenius plot of the data in columns 4 and 5 of table 2. These values and uncertainties are given in table 3.

Table 3. Pre-exponential and activation parameters for diffusion of Cs in IG-110 graphite between 1100K and 1300K.

Material	FP	D_0 (m^2/s)	$\pm\Delta\ln D_0$	E (J/mol)	$\pm\Delta E$ (J/mol)
IG-110	Cs	1.0×10^{-7}	2.90	1.1×10^{5}	2.8×10^{4}

We have thus measured diffusion coefficients of Cs in IG-110 in the temperature range of 1100-1300K by using the release method and ICP-MS. We have used a carbon aerosol laden helium-jet system to transport Cs diffusing from a heated graphite sphere to an online ICP-MS to determine release rates and cumulative release in real time. We have obtained:

$$D_{Cs} = 10^{-7}\exp\left(\frac{-1.1\times10^{5}\,(J/mol)}{RT}\right)\left(m^2/s\right)$$

The method we have developed is easily adaptable to measure diffusion of other fission products or multiple fission products, diffusion in other types of graphite or other materials of interest, and the effects of oxidation and other chemical or physical stresses on diffusion behavior.

The full details of our work on diffusion of Cs and Iodine in IG-110 and NBG-18 in spherical and cylindrical compacts are described in the following publications:

- Carter, L.M., Brockman, J.D., Loyalka, S.K. Robertson, J.D., "Measurement of Cs diffusion coefficients in IG-110 graphite." J. Nuc. Materials **460**, 30-36 (2015)
- Carter, L.M., Brockman, J.D., Robertson, J.D. Loyalka, S.K., "ICP-MS Measurement of Cs diffusion coefficients in NBG-18 graphite," J. Nuc. Materials**466**, 402-408 (2015)
- Carter, L.M., Brockman, J.D. Loyalka, S.K., Robertson, J.D, "Calibration of a system for measurements of diffusion coefficients of fission products in HTGR/VHTR core materials," J. Radioanal Nucl Chem DOI 10.1007/s10967-015-4633-0 (2015)
- Carter, L.M., Brockman, J.D., Robertson, J.D. Loyalka, S.K.,"ICP-MS Measurement of Iodine Diffusion in IG-110 graphite for HTGR/VHTR" (Submitted, under review)
- Carter, L.M., Brockman, J.D., Robertson, J.D. Loyalka, S.K., "Diffusion of Cesium and Iodine in Compressed IG-110 Graphite Compacts ," (Submitted, under review)

We have also constructed a detailed computational model for fission product diffusion in porous nuclear fuels and materials. The details of this work are described in,

- Simones, M.P., Reinig, M.L., and Loyalka, S.K., "A Mathematical Model for the Release of Noble Gas and Cs from Porous Nuclear Fuel Based on VEGA 1&2 Experiments," *Journal of Nuclear Mater DOI:10.1016/j.jnucmat.2014.01.050 (2014)*

We found that our experiments were adequately described by the simpler equations and models, and the use of the above model did not become necessary.

In summary, we have obtained the following experimental results:

Table I. Summary of Experimental Results

FP	Material	Temp Range (K)	Method	Diffusion Coefficient D (m^2/s)
Cs	IG-110	1100-1300	Release	$1.0\times10^{-7}\,Exp\left[-1.1\times10^{5}\,(J/mol)/RT\right]$
Cs	NBG-18	1090-1395	Infusion/Release	$1.0\times10^{-1}\,Exp\left[-1.23\times10^{5}\,(J/mol)/RT\right]$
I	IG-110	873-1270	Release	$\sim 1.6\times10^{-11}$

We are continuing to do additional work in the post project period to acquire new diffusion data on a well selected combination of fission products (as well as their surrogates) into graphite and other structural material samples.

Task 2: Adsorption Measurements

The understanding and computation of Fission Product (FP) retention or release, requires measurements of adsorption isotherms. We explored several designs of the fission product experiment as discussed in previous reports.

Initial Thermogravimetric Analysis Approach

We first considered a Thermogravimetric Analyzer (TGA) with Temperature Programmed Desorption (TPD). A diagram of the TGA is shown in Figure below. A small graphite sample will have a thin film of silver sputtered onto its surface. This layer will then be removed using a glass/diamond blade on a micrometer. The very thin slices of graphite saturated with silver will be placed in a TGA and the temperature increased. Using the very sensitive mass measuring capabilities of the TGA, we were expecting to see a spike in mass change during the heating period. This spike is the point of analysis when using the TPD method.

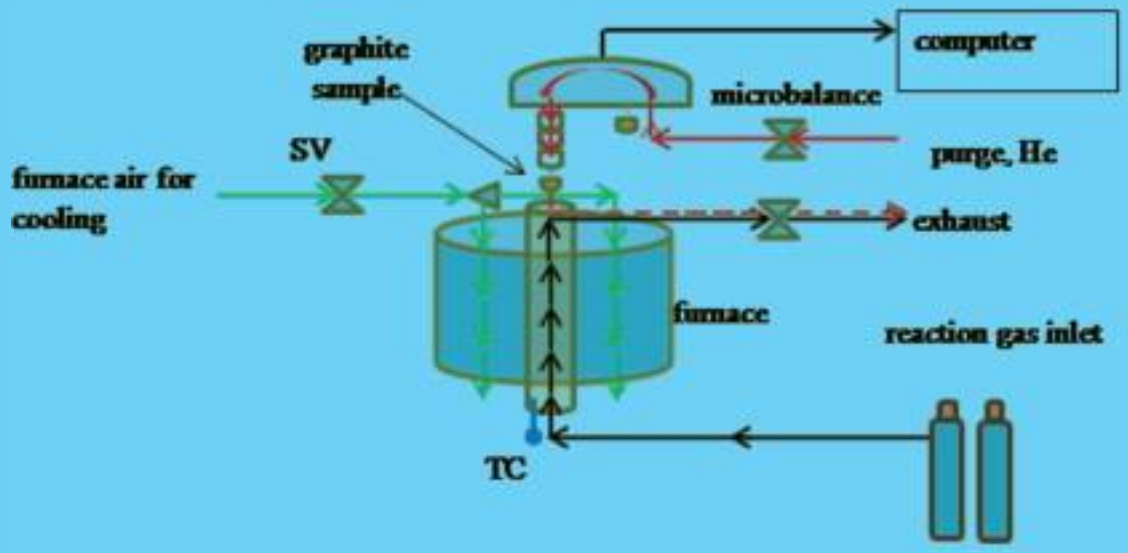

Figure 1: Schematic of the TGA and placement of the graphite sample.

Modified Thermogravimetric Analysis Approach

In considering (sensitivity) issues with the first setup, we modified our approach. In the Figure 1, where the graphitic sample is placed, there is a small quartz bulb. The quartz bulb actually houses the graphite sample and a small amount of silver powder. The wire attached to the TGA's microbalance passes through the top of the bulb and attaches to the graphite sample. Only the graphite sample is suspended from the microbalance wire, not the powder or the bulb. It is expected that the silver will form vapor, ensconcing the graphite. As the silver particles sorb onto the surface of the graphite sample, the TGA will detect the change in mass.

Knudsen Cell Approach

Neither of the above techniques, and some variations on these, yielded any useful results. We then decided to adopt the techniques of Hilpert and Myers & Bell. Both parties used a high temperature vacuum Knudsen Cell in conjunction with a mass spectrometer in their studies of older graphites. This combined technique had been useful in discovering binding energies and volatilities (and hence adsorption isotherms) associated with organic materials, and has become known as Knudsen Effusion Mass Spectrometry (KEMS). A detailed diagram of the KEMS apparatus we are currently using (for measurements of Ag and Sr adsorption on IG-110 and NBG-18 at NASA-Glenn research center) is shown in fig. 2.

The present technique uses graphite characterization using Fourier Transform Infrared Spectroscopy (FTIR) and Brunauer-Emmett-Teller surface area (BET) measurements. Sample preparation involved the use of aqueous solutions of nitrate salts on graphite powders followed by drying/vacuum sealing and decomposition at >100°C for a week or more. Surface mass concentration measurements of FPs were performed on the samples, along with calibration of KEMS with measurements with silver, and then acquisition of vapor pressure data at different temperatures on the samples. We also obtain post KEMS measurements of FP concentration on the used samples using INAA at MURR.

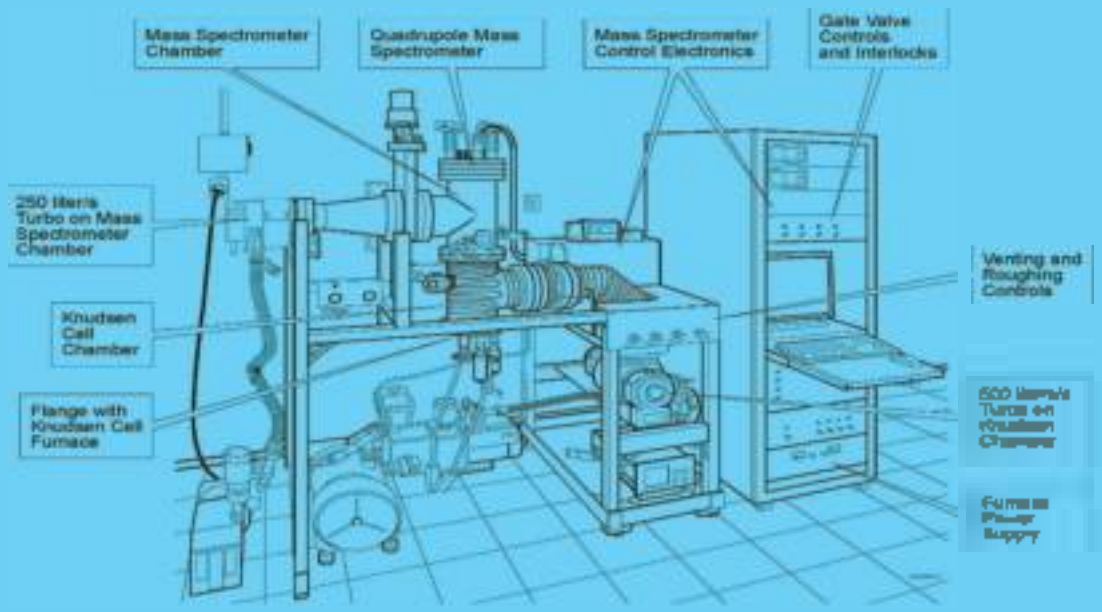

Figure 2. A detailed diagram of the KEMS system at NASA-Glenn (we are presently working in collaboration with Dr. Nathan Jacobson at NASA-Glenn).

The NASA Glenn Research Center (GRC) has two different available KEMS systems, with quadrupole and magnetic sectors. Preliminary studies of the mass spectrometer properties determined that using a quadrupole would allow for a higher sensitivity to count rate. In contrast, the magnetic sector provides great isolation of exact mass to charge ratios. This has allowed the comparison of tabulated values for silver and strontium available in the literature.

We fully characterized and calibrated the KEMS system with the mass spectrometer at NASA-GRC. It was determined that the KEMS output signaling was too distorted by noise for satisfactory measurements. This has been now addressed, and is not an issue moving forward. We have determined the mass and concentrations necessary to boost the signal to noise ratio, and more experiments will be performed. A calibration curve for Silver is shown below in Fig. 3:

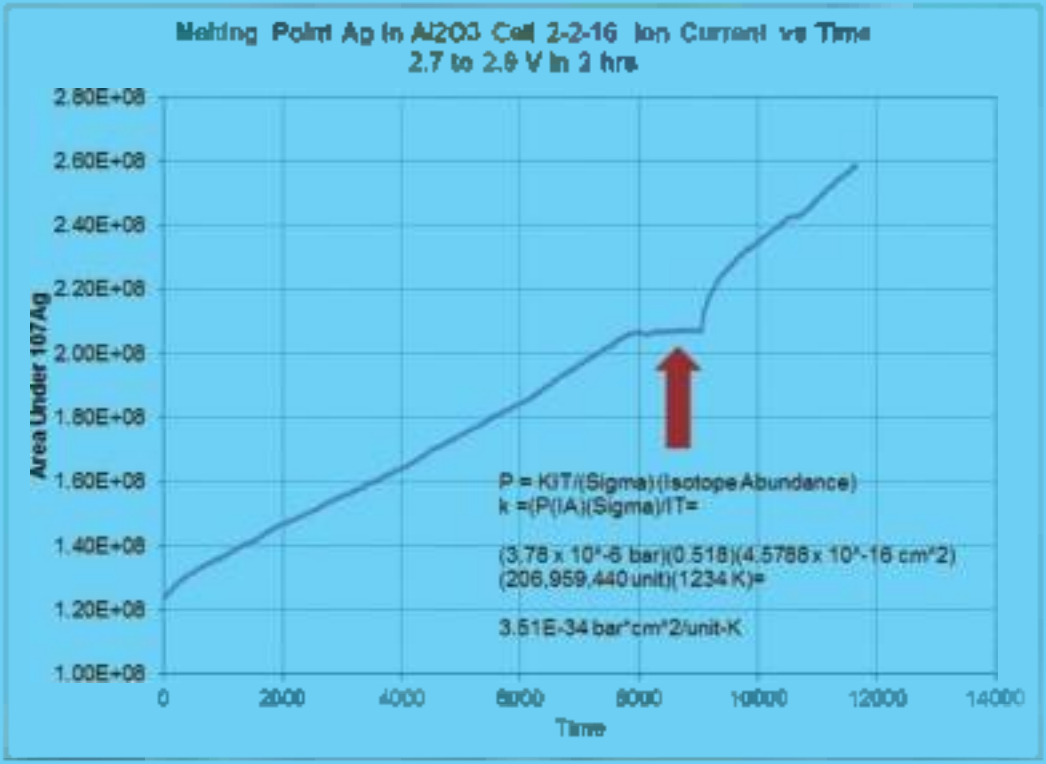

Figure 3: A sample calibration run resulting in the calibration curve and calibration constant 'k'. This experiment was Ag in Aluminum Oxide cell. The resulting factor is key to convert measured intensity to pressure.

The planned scope of the summer 2016 visit to NASA-GRC, when the instrument becomes available again, is characterization of NBG-18 and IG-110 with strontium and silver.

Of additional interest, it has come to our attention that previous and current experiments elucidate oxygenation of Sr-C and Cs-C bonds, implying nitrate disassociation heating. Hilpert noted that the metal favored binder residue locations rich in oxygen. Through characterization of the graphite using BET and FTIR, we intend to isolate this effect for both Ag and Sr. We have also reviewed the theoretical work which

indicates lower binding energies than experimentally observed. Verification of the Sr-O-C bonding will be of great consequence, and will be clarified as a side result of the experiment.

Although we do not have specific data to report at this time, we will submit a supplementary report to DOE upon completion of fall 2016 measurements and related analysis.

Task3: Dust-Gas Interactions

Discussion

Our focus in this task is on modeling of dust-Fission Product (FP) interactions, and thus to provide basis for computation of dust facilitated FP transport. Dust can be generated by abrasion, gas to particle conversion, and degradation of insulation, etc. Some experiments, have indicated that the carbonaceous dust particles produced by graphite abrasion can be highly irregular, and this may be true of particles generated by other mechanisms too. It has been also found that graphite particles can also be highly porous with very large surface areas that may make dust facilitated FP transport a major factor. Since the FP interactions with the dust can occur while the dust is on a surface as well as in suspension, we will address both these phenomena.

For the larger particles (as compared to the FP mean free path), the fundamental approach that we are taking is the Green's function technique for the diffusion equation. Our basic approach considers the diffusion of a FP in a background gas (helium for example) around a particle (or a collection of particles). We also will consider particles with a specified porous structure. We convert the diffusion equation to a system of boundary integral equations by using a singularity subtraction technique and then solving the resulting system of equations, thereby obtaining results for absorption rates of the FP on the particle. The technique has been applied successfully to that of (hindered) iodine evaporation from both single particles, as well as particle ensembles. We are developing and exploring applications of this technique further for linear chains of particles and other agglomerates and shapes. Additionally, we are using the results to obtain representative shape factors that define the absorption rates for spheres that have the same absorption as actual particles. Given the complexity of these shapes, the use of shape factors in these scenarios may not suffice and our actual computations may be of greater value.

We recognize that the diffusion equation alone would not suffice in the vicinity of surface pores, for smaller particles, and for small spaces in an agglomerate, the mean free path of the FP molecules becomes comparable to pore and particle size. To address these cases we are exploring the linear Boltzmann Equation through the standard Monte Carlo technique using MCNP as well as our own programs for the Direct Simulation Monte Carlo technique for the non-linear Boltzmann equation. We describe below some details of our work.

One Speed Transport Calculations of Condensation Rates and Shape Factors

The problem of condensation on particles as based on the Linear Boltzmann Equation and associated boundary conditions has been discussed in some detail by Williams and Loyalka (Aerosol Science. Theory and Practice, 1991). We assume that vapor (gaseous phase) molecules that strike the particles condense fully, and that the molecules re-evaporate from the particle surfaces according to the saturation density (this is consistent with the actual case of re-evaporation of the molecular distribution as a Maxwellian). Thus considering an ensemble of aerosol particles, we can describe the transport of the vapor in the gas phase by the equations:

$$\Omega \cdot \frac{\partial}{\partial r}\psi(r,\Omega) = -\psi(r,\Omega) + \frac{1}{4\pi}\int \psi(r,\Omega')d\Omega'$$

$$\psi(r_s,\Omega) = \frac{n_s}{4\pi}, \quad \Omega \cdot n_s(r_s) > 0$$

$$\lim_{r\to\infty}\psi(r,\Omega) = \frac{n_\infty}{4\pi}$$

The main quantities of interest here are the local and total condensation rates on each particle are respectively defined as:

$$J(r_s) = -\int \Omega \cdot n_s(r_s)\psi(r_s,\Omega)d\Omega$$

And,

$$\mu = \int J(r_s)\,dr_s$$

Here r is the non-dimensionalized distance, measured in terms of a mean free path ℓ and n_s and n_∞ are, respectively the molecular saturation density and density far away from the surface in the bulk of the gas phase. Also, ψ is the molecular distribution function (that is number of molecules per unit volume per steradian, or the molecular "flux", number of molecules per unit area per steradian per sec, as the speed here is fixed). $n_s(r_s)$ is the unn normal vector directed from a body towards and in the gas phase at the surface point r_s.

We assume that the particles are highly absorbing in that a molecule incident on a particle is fully absorbed (in the computations we do so by assigning an arbitrarily large molecular absorption cross-section to the particles), but that an evaporation as specified by Eqn. (2), and directed in to the gas, is maintained at the particle surface. For the present, we have also assumed, that all particles are similar, and that the particle surfaces are homogeneous.

Here we define the mean free path (m) as:

$$\ell = 1/\Sigma_t$$

Where Σ_t is the total molecular cross-section (molecule/background), and is expressed in terms of the diffusion coefficient D (m^2/s) of the molecules (in the background gas as):

$$\Sigma_t = \frac{\bar{v}}{3D}$$

Here $\bar{v}$ is the mean or some specific molecular speed (e.g. in the one speed model one has a choice), which we take to be

$$\bar{v} = \left(\frac{8kT}{\pi m}\right)^{1/2}$$

Where m is the molecular mass, k is the Boltzmann Constant, and T is the temperature. Thus we have,

$$\ell = \frac{3\pi^{1/2}}{4} 2D\left(\frac{m}{2kT}\right)^{1/2} = \frac{3D}{\bar{v}}$$

Note that the factor $3\pi^{1/2}/4$ appearing here is of order 1. Alternate choices of the "mean" speed can lead to different factors, but the main point is to relate the mean free path to the diffusion coefficient so then the results can be compared well with the solutions of the advanced molecular models and also the full linear Boltzmann equation.

In order to apply the Monte Carlo to the above problem, we must truncate the problem geometry at a finite radius. Thus, at first we consider a finite geometry problem instead:

$$\Omega \cdot \frac{\partial}{\partial \mathbf{r}} \psi(\mathbf{r}, \mathbf{\Omega}) = -\psi(\mathbf{r}, \mathbf{\Omega}) + \frac{1}{4\pi} \int \psi(\mathbf{r}, \mathbf{\Omega}') d\mathbf{\Omega}'$$

$$\psi(\mathbf{r}_1, \mathbf{\Omega}) = \frac{n_1}{4\pi}, \quad \mathbf{\Omega} \cdot \mathbf{n}_r(\mathbf{r}_1) > 0$$

$$\psi(\mathbf{r}_2, \mathbf{\Omega}) = \frac{n_\infty}{4\pi}$$

And we let the radius $R_2 = |\mathbf{r}_2|$ be considerably large to encompass all the particles, and we compute the condensation rate in the limit of very large R_2.

Actually, since the transport equation here is linear, without loss of generality, we can set,

$$\psi(\mathbf{r}, \mathbf{\Omega}) = \frac{n_1}{4\pi} + (n_\infty - n_1)\hat{\psi}(\mathbf{r}, \mathbf{\Omega})$$

And obtain $\tilde{\psi}(\mathbf{r},\boldsymbol{\Omega})$ by solving the equation,

$$\boldsymbol{\Omega}\cdot\frac{\partial}{\partial \mathbf{r}}\tilde{\psi}(\mathbf{r},\boldsymbol{\Omega}) = -\tilde{\psi}(\mathbf{r},\boldsymbol{\Omega}) + \frac{1}{4\pi}\int \tilde{\psi}(\mathbf{r},\boldsymbol{\Omega}')d\boldsymbol{\Omega}'$$

$$\tilde{\psi}(\mathbf{r}_s,\boldsymbol{\Omega}) = 0, \quad \boldsymbol{\Omega}\cdot\mathbf{n}_s(\mathbf{r}_s) > 0$$

$$\tilde{\psi}(\mathbf{r}_2,\boldsymbol{\Omega}) = \frac{1}{4\pi}$$

And the tabular condensation rate results that we report later correspond to results for the quantity,

$$\dot{u} = \int \dot{J}(\mathbf{r}_s)\, d\mathbf{r}_s$$

Where,

$$\dot{J}(\mathbf{r}_s) = -\int \boldsymbol{\Omega}\cdot\mathbf{n}_s(\mathbf{r}_s)\tilde{\psi}(\mathbf{r}_s,\boldsymbol{\Omega})\, d\boldsymbol{\Omega}$$

From a mathematical point of view, solving the above Eqns. with many particles, and the outer radius going to the infinity in the limit, is the main focus of this study.

Since our goal is to model vapor physics in the vicinity of aerosols of the type typically found among VHTR dust, we created two token geometries—a nonlinear aerosol chain, and an aerosol agglomeration. Of course there are many more possible geometries, recent research has shown that typically these aerosols will exist in chains of varying length, or in 'clumps' of varying size.

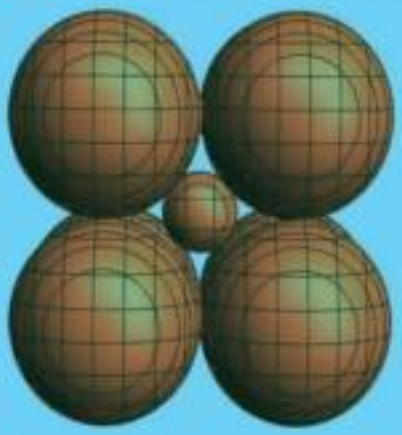

For computational purposes, we have essentially considered the problem as defined by the equations and computed results using the Monte Carlo method. We used two different programs:

- Our own specialized program written wnh in Mathematica 10.3, where we have used Mathematica's functionality and visualization abilities (we will later use this program to explore dependence of results on arbitrary surfaces conditions).
- MCNP-6.1.1, the Monte Carlo N-Particle (MCNP) transport Code, with several basic modifications that allow this code to be bootstrapped (with some stipulations) for mass-transport calculations, by exploiting the nature of the MCNP code as a Linear Boltzmann transport simulator.

We do not discuss the details of these techniques here, but regarding the use of the MCNP-6 we note that we created and used different molecule-background cross-section sets for the molecules in the gas phase and the interiors of the particles. We also increase the absorption (and hence the total) cross-section to an arbitrary large value in the interior of the particle. MCNP also requires some care in computing the molecular current. We used a F1 (flux) tally (see the MCNP user manual for more in depth explanations of nomenclature) across all surfaces of interest, and a cosine tally with two angular bins corresponding to ingoing and outgoing currents at the surfaces (the way the problem is defined, the outgoing current on the particles is zero). The net current was obtained as difference between these, and the condensation rate was obtained as an integral of the net current over the particle surface. We did not tally for local condensation rates as in the present work we have focused on the total condensation rates on each particle in the chain of particles and the agglomerate.

We carried out extensive calculations to determine the shape factors of various aerosol geometries Our main conclusion from the study was that complex aerosol geometries greatly hinder condensation rates, and that single speed calculations come very close to 'good enough' for many practical purposes. A paper relating to this work has been published, and full details can be found there.

We have extended our own Monte Carlo code (implemented in the Wolfram Language and ANSI-C) to the Linear Boltzmann Equation with full speed and mass ratio dependence, and verified the results against those reported for a single sphere (numerical results for this case had been reported in the literature in 1989). We again find that the condensation rates (and hence shape factors) are relatively insensitive to the mass ratio (background/vapor, as long as the mean free path is defined in terms of the vapor diffusion coefficient). A manuscript based on this work is in preparation.

We have published a paper on the shape factors in the continuum limit by using the Green's Function Method, and we have reported several results on both the local and global condensation rates. We have also carried out extensive additional work on agglomerates with a fairly large number of particles. In doing so, we have used many advanced computational techniques. A manuscript based on this work is in preparation.

Some work we carried out in the above conjunction is related to benchmarking of Monte Carlo calculations against an interesting 3-D source problem, on a semi-infinite domain for which analytical solution were available.

The following publications provide the details of some of the work noted above:

1. Smith, Z., and Loyalka, S. K., "Numerical Solutions of the Poison Equation: Condensation/Evaporation on Arbitrarily Shaped Aerosols," Nuclear Science and Engineering 176, 154-166 (2014)

2. Jeong, J., White, N.E., and Loyalka, S. K., "Three Dimensional Transport Theory: Evaluation of Analytical Expressions of Williams and verification of MCNP," Annals of Nuclear Energy, 86, 80-87 (2015)

3. White, N.E., and Loyalka, S. K., "Computation of Fission Product Condensation on Chainlike Aerosols and Agglomerates," Nuclear Science and Engineering 181, 318-330 (2015)

We have completed very substantial additional work, and two manuscripts are in preparation:

1. White, N. E. and Loyalka S. K., "Numerical Solutions of the Poison Equation: Condensation/Evaporation on Arbitrarily Shaped Aerosols- II"

2. White, N.E., Tompson, R. and Loyalka, S. K., "Computation of Fission Product Condensation on Chainlike Aerosols and Agglomerates: The Linear Boltzmann Equation"